Inorg. Chem. **2008**, *47*, 3955−3957

3D Metal−Organic Frameworks Based on Elongated Tetracarboxylate Building Blocks for Hydrogen Storage

Liqing Ma,[†] Jeong Yong Lee,[‡] Jing Li,[‡] and Wenbin Lin*[,†]

Department of Chemistry, CB#3290, University of North Carolina, Chapel Hill, North Carolina 27599, and Department of Chemistry and Chemical Biology, Rutgers University, Piscataway, New Jersey 08854

Received February 29, 2008

Two 3D metal−organic frameworks (MOFs) with a new biphenol-derived tetracarboxylate linker and Cu^{II} and Zn^{II} metal-connecting points were synthesized and characterized by single-crystal X-ray crystallographic studies. The two isostructural MOFs exhibit distorted PtS network topology and show markedly different framework stability. The porosity and hydrogen uptake of the frameworks were determined by gas adsorption experiments.

A wide range of applications can be envisioned for metal−organic frameworks (MOFs) owing to their modular nature and mild synthetic conditions, and as a result, there is an immense current research interest in designing functional MOFs.[1–7] Well-designed MOFs have, for example, already found applications in nonlinear optics,[5] gas storage,[8–12] and catalysis.[13–17] Carboxylate linkers, including dicarboxylate, tricarboxylate, and tetracarboxylate ligands, are among the most important and widely used bridging ligands for constructing stable MOFs with permanent porosity. Particularly, Yaghi and co-workers have reported highly porous IRMOFs built from linear dicarboxylate groups with varied dimensions.[18] Highly porous MOFs have also been built from tricarboxylate linkers such as 4,4′,4″-*s*-triazine-2,4,6-triyltribenzoate,[19] as well as tetracarboxylate linkers such as 3,3′,5,5′-azobenzenetetracarboxylate.[20] Recently, Schröder and co-workers have synthesized a set of highly porous MOFs utilizing different sizes of tetracarboxylate linkers such as biphenyl-3,3′,5,5′-tetracarboxylate, terphenyl-3,3″,5,5″-tetracarboxylate, and quaterphenyl-3,3‴,5,5‴-tetracarboxylate, all of which have shown high hydrogen adsorption capacity.[10]

We have recently constructed a number of highly porous MOFs using bridging ligands derived from 1,1′-bi-2-naphthol, some of which have shown promising applications in gas storage and asymmetric heterogeneous catalysis.[9,13,16,21] In search of new bridging ligands containing orthogonal functional groups, we have become interested in designing new bridging ligands based on the biphenol system. The dihydroxy groups in the biphenol system can be either protected with an alkyl group or unmasked for further modification to lead to functional MOFs. Herein we report the design of a new biphenol-based tetracarboxylic acid and the construction of two isostructural MOFs with distorted PtS network topology using the new tetracarboxylate linker. The copper framework exhibits a high surface area and shows a good hydrogen uptake capacity of ∼0.8 wt % at 77 K under 1 atm.

3,3′,5,5′-Tetrabromobiphenol (**1**) and its ethoxy derivative (**2**) were prepared according to the literature procedures.[22] The ligand precursor 2,2′-diethoxylbiphenyl-3,3′,5,5′-tetra-

* To whom correspondence should be addressed. E-mail: wlin@unc.edu.
† University of North Carolina.
‡ Rutgers University.

(1) Moulton, B.; Zaworotko, M. J. *Chem. Rev.* **2001**, *101*, 1629.
(2) Eddaoudi, M.; Moler, D. B.; Li, H.; Chen, B.; Reineke, T. M.; O'Keeffe, M.; Yaghi, O. M. *Acc. Chem. Res.* **2001**, *34*, 319.
(3) James, S. L. *Chem. Soc. Rev.* **2003**, *32*, 276.
(4) Batten, S. R.; Robson, R. *Angew. Chem., Int. Ed.* **1998**, *37*, 1461.
(5) Evans, O. R.; Lin, W. *Acc. Chem. Res.* **2002**, *35*, 511.
(6) Férey, G.; Mellot-Draznieks, C.; Serre, C.; Millange, F. *Acc. Chem. Res.* **2005**, *38*, 217.
(7) Yaghi, O. M.; O'Keeffe, M.; Ockwig, N. W.; Chae, H. K.; Eddaoudi, M.; Kim, J. *Nature* **2003**, *423*, 705.
(8) Rosi, N. L.; Eckert, J.; Eddaoudi, M.; Vodak, D. T.; Kim, J.; O'Keeffe, M.; Yaghi, O. M. *Science* **2003**, *300*, 1127.
(9) Kesanli, B.; Cui, Y.; Smith, M. R.; Bittner, E. W.; Bockrath, B. C.; Lin, W. *Angew. Chem., Int. Ed.* **2005**, *44*, 72.
(10) Lin, X.; Jia, J.; Zhao, X.; Thomas, K. M.; Blake, A. J.; Walker, G. S.; Champness, N. R.; Hubberstey, P.; Schroder, M. *Angew. Chem., Int. Ed.* **2006**, *45*, 7358.
(11) Dincă, M.; Yu, A. F.; Long, J. R. *J. Am. Chem. Soc.* **2006**, *128*, 8904.
(12) Ma, S.; Sun, D.; Ambrogio, M.; Fillinger, J. A.; Parkin, S.; Zhou, H. *J. Am. Chem. Soc.* **2007**, *129*, 1858.
(13) Wu, C.; Lin, W. *Angew. Chem., Int. Ed.* **2007**, *46*, 1075.
(14) Dybtsev, D. N.; Nuzhdin, A. L.; Chun, H.; Bryliakov, K. P.; Talsi, E. P.; Fedin, V. P.; Kim, K. *Angew. Chem., Int. Ed.* **2006**, *45*, 916.
(15) Lin, W. *J. Solid State Chem.* **2005**, *178*, 2486.
(16) Wu, C.; Hu, A.; Zhang, L.; Lin, W. *J. Am. Chem. Soc.* **2005**, *127*, 8940.
(17) Hu, A.; Ngo, H. L.; Lin, W. *J. Am. Chem. Soc.* **2003**, *125*, 11490.
(18) Eddaoudi, M.; Kim, J.; Rosi, N.; Vodak, D.; Wachter, J.; O'Keefe, M.; Yaghi, O. M. *Science* **2002**, *295*, 469.
(19) Sun, D.; Ma, S.; Ke, Y.; Collins, D. J.; Zhou, H. *J. Am. Chem. Soc.* **2006**, *128*, 3896.
(20) Liu, Y.; Eubank, J. F.; Cairns, A. J.; Eckert, J.; Kravtsov, V. C.; Luebke, R.; Eddaoudi, M. *Angew. Chem., Int. Ed.* **2007**, *46*, 3278.
(21) Cui, Y.; Ngo, H. L.; White, P. S.; Lin, W. *Chem. Commun.* **2003**, 994.

10.1021/ic8003855 CCC: $40.75
Published on Web 04/17/2008

Scheme 1

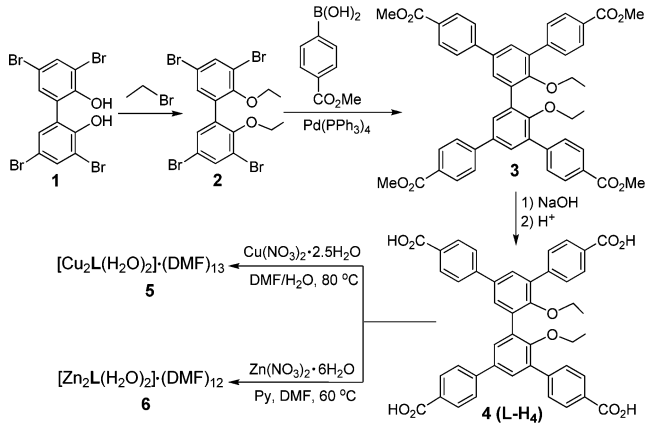

kis(4-methylbenzoate) (**3**) was synthesized by Suzuki coupling of 3,3′,5,5′-tetrabromo-2,2′-diethoxylbiphenyl (**2**) with 4-(methoxycarbonyl)phenylboronic acid. Biphenol-derived tetracarboxylic acid **L-H$_4$** was synthesized by hydrolysis of **3** (Scheme 1). The copper complex $[Cu_2\mathbf{L}(H_2O)_2]\cdot 13DMF$ (**5**) was synthesized by the reaction of **L-H$_4$** with copper nitrate in a *N*,*N*-dimethylformamide (DMF)/H_2O solvent mixture with the addition of a small amount of a diluted aqueous HCl solution at 80 °C, whereas the zinc complex $[Zn_2\mathbf{L}(H_2O)_2]\cdot 12DMF$ (**6**) was obtained by reacting **L-H$_4$**with zinc nitrate in DMF in the presence of pyridine at 60 °C.

Thermogravimetric analyses (TGA) of **5** show a significant weight loss of 53.6% in the temperature range of 25−200 °C, corresponding to 2 coordinated H_2O molecules and 13 DMF molecules residing in the open channels of **5** (expected 53.8%). TGA for **6** reveal a weight loss of 51.5% in the temperature range of 25−200 °C, corresponding to 2 coordinated H_2O molecules and 12 DMF molecules per formula unit (expected 51.7%). Powder X-ray diffraction patterns of bulk samples of **5** and **6** match those simulated from their single-crystal structures, indicating their phase purity. The powder X-ray diffraction patterns of **5** and **6** match perfectly, suggesting their isostructural relationship.

Single-crystal X-ray diffraction studies showed that **5** and **6** are isostructural, crystallizing in monoclinic space group *C*2/*c*.[23] Only the structural details of **5** are described here. There are four crystallographically independent Cu atoms, one full **L**, two half **L** ligands, and four coordinated water molecules in each asymmetric unit. The four carboxylate groups from four different **L** ligands bridge a pair of Cu^{II} ions to form a $[Cu_2(O_2CR)_4]$ paddlewheel unit, with the axial positions occupied by coordinated water molecules (Figure 1). Each Cu^{II} ion is thus coordinated to four carboxylate and one water O atom in a square-pyramidal geometry. The **L** ligands link the four crystallographically independent Cu^{II} ions to form three crystallographically independent $[Cu_2(O_2CR)_4]$ paddlewheel units (Cu1−Cu1, Cu2−Cu3, and Cu4−Cu4). These Cu_2 paddlewheel units (shown as squares in Figure 1b) are interconnected by the three independent **L** ligands (simplified as distorted tetrahedra in Figure 1b) to lead to a very open 3D framework with distorted PtS topology (Figure 2a). Three different tetrahedra shown in gray, aqua, and pink colors represent the three crystallographically independent **L** ligands, which have distinct dihedral angles of 51.1° (blue), 54.4° (gray), and 89.3° (red) for the central biphenyl rings, respectively (Figure 2a). The three independent copper paddlewheels are also depicted in three different colors: red, blue, and green (Figure 2a). Several MOFs with PtS network topology have been reported in the literature.[24–28]

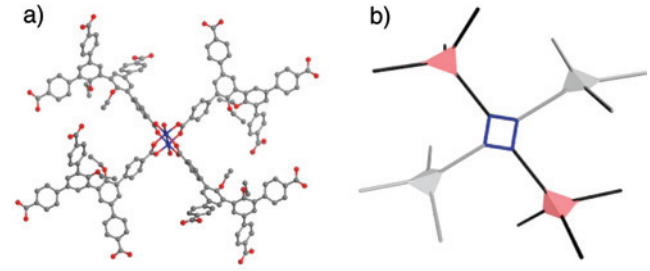

Figure 1. (a) Portion of the crystal structure of **5** showing coordination environments of Cu^{II} ions in the $[Cu_2(O_2CR)_4]$ paddlewheel unit with coordinated axial H_2O molecules: C, gray; Cu, blue; O, red. H atoms are omitted for clarity. (b) Schematic representation of the same portion of the structure of **5** shown in part a, with the $[Cu_2(O_2CR)_4]$ paddlewheel unit depicted as a blue square and the four carboxylate groups of each **L** ligand represented by a tetrahedron.

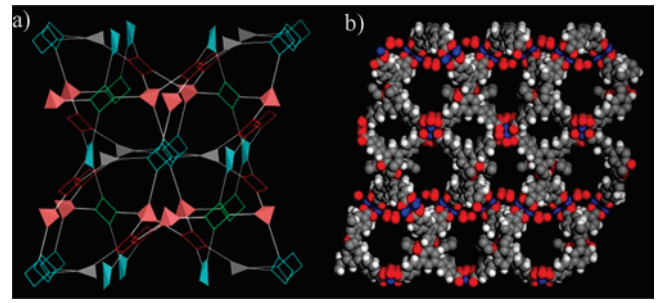

Figure 2. (a) Scheme representation of the 3D networks of **5** as viewed down the *c* axis. (b) Space-filling representation of the structure of **5** as viewed perpendicular to the (1 1 0) plane. Guest molecules are omitted for clarity.

(22) Gómez-Lor, B.; Echavarren, A. M.; Santos, A. *Tetrahedron Lett.* **1997**, *38*, 5347.

(23) All single-crystal X-ray diffraction data were measured at 296 K on a Bruker SMART Apex II CCD-based X-ray diffractometer system equipped with a Mo-target X-ray tube (λ = 0.710 73 Å). Crystal data for **5**: monoclinic, space group *C*2/*c*, a = 41.483(7) Å, b = 41.783(7) Å, c = 30.968(7) Å, α = 90°, β = 109.895(11)°, γ = 90°, V = 50 472(16) Å^3, Z = 8, ρ_{calcd} = 0.462 g/cm^3, μ(Mo Kα) = 0.357 mm^{-1}. Data/restraints/parameters: 24 765/866/874, R1 [$I > 2\sigma(I)$] = 0.0703, wR2 = 0.1654, R1 (all data) = 0.1634, wR2 (all data) = 0.1774, GOF = 0.707 (0.702 restrained). Crystal data for **6**: monoclinic, space group *C*2/*c*, a = 41.812(2) Å, b = 41.815(2) Å, c = 31.156(2) Å, α = 90°, β = 109.607(3)°, γ = 90°, V = 51 314(4) Å^3, Z = 8, ρ_{calcd} = 0.456 g/cm^3, μ(Mo Kα) = 0.394 mm^{-1}. Data/restraints/parameters: 25 746/1014/884, R1 [$I > 2\sigma$(I)] = 0.0547, wR2 = 0.1481, R1 (all data) = 0.1043, wR2 (all data) = 0.1519, GOF = 0.973 (0.966 restrained).

(24) Chen, B.; Eddaoudi, M.; Reineke, T. M.; Kampf, J. W.; O'Keeffe, M.; Yaghi, O. M. *J. Am. Chem. Soc.* **2000**, *122*, 11559.

(25) Abrahams, B. F.; Hoskins, B. F.; Michail, D. M.; Robson, R. *Nature* **1994**, *369*, 727.

(26) Carlucci, L.; Ciani, G.; von Gudenberg, D. W.; Proserpio, D. M. *New J. Chem.* **1999**, *23*, 397.

(27) Reineke, T. M.; Eddaoudi, M.; O'Keeffe, M.; Yaghi, O. M. *Angew. Chem., Int. Ed.* **1999**, *38*, 2590.

(28) Natarajan, R.; Savitha, G.; Dominiak, P.; Wozniak, K.; Moorthy, J. N. *Angew. Chem., Int. Ed.* **2005**, *44*, 2115.

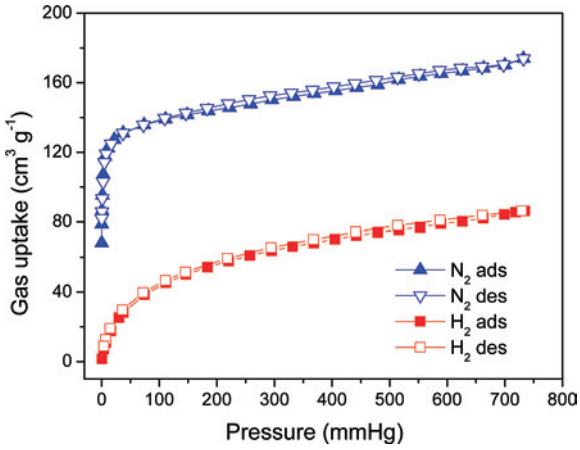

Figure 3. N_2 and H_2 sorption isotherms measured for desolvated **5** at 77 K (ads = adsorption; des = desorption).

As reported in the literature examples,[24,28] porous framework structures with open channels are expected of **5** and **6** because of the use of elongated tetracarboxylate bridging ligands. Space-filling models of crystal structures of **5** and **6** indicate the presence of open channels of ~9 Å × 9 Å in dimensions that run perpendicular to the (1 1 0) and (1 0 −1) planes (Figure 2b). PLATON calculations showed that the solvent-accessible volume in **5** is about 37 735 Å^3 out of the unit cell of 50 472 Å^3, which constitutes ~74.8% of the total volume of the crystal. A very similar void space of ~75.2% was found for **6**.

The porosity of **5** and **6** was also characterized by N_2 adsorption experiments at 77 K (Figure 3). Both samples were immersed in acetone for 1 h to have all of the included DMF molecules exchanged, dried in an argon flow for 1 h, and then evacuated at 60 °C for 13 h. The N_2 adsorption isotherm of **5** shows reversible type I behavior, indicating the retention of the microporous structures after removal of the solvent molecules in the channels. **5** exhibits a Barrett−Joyner−Halenda (BJH) cumulative adsorption surface area of 1755 m^2/g (and a Langmuir surface area of 733 m^2/g). **5** has a pore volume of 0.42 cm^3/g and a pore size of 8 Å as calculated by the BJH method. Although the solvent-accessible void volume of **6** calculated by PLATON is very similar to that of **5**, the N_2 adsorption isotherms of **6** showed essentially no N_2 uptake. However, CO_2 adsorption isotherms for **6** showed a modest Langmuir surface area of 252 m^2/g. The different surface areas observed for **6** with different adsorbates indicated that its framework might have become distorted to lead to partially blocked channels upon the removal of solvent molecules.[29] In contrast, the framework structure of **5** is more stable and does not distort upon solvent removal.

Because of the high microporosity of **5**, we have performed hydrogen uptake experiments at 77 K. A hydrogen uptake of 0.8 wt % was obtained for **5**. Consistent with the partial collapse of its framework structure, **6** has a much lower hydrogen uptake of only 0.2 wt % under the same conditions.

We have also carried out solid-state fluorescence measurements on free ligand **L-H$_4$** and **6**. Both compounds show similar emission peaks of 402 nm under excitation of 350 nm (Figures S11 and S12 in the Supporting Information). These results indicate that the electronic structures of the **L** ligand remain essentially unchanged upon formation of the MOF.

In summary, we have synthesized copper and zinc 3D open frameworks based on biphenol-derived tetracarboxylate building blocks. The carboxylate groups link pairs of metal centers to form [$M_2(O_2CR)_4$] paddlewheel units, which are further connected by the biphenol moieties to lead to open frameworks with distorted PtS topology. The copper open framework **5** is highly porous with a hydrogen uptake capacity of 0.8 wt %. The dihydroxy groups that can be unmasked from the **L** ligand shall allow its further derivatization for the construction of new functional porous MOFs.

Acknowledgment. W.L. thanks the NSF (Grant DMR-0605923) for financial support.

Supporting Information Available: Experimental procedures, TGA results, X-ray powder diffraction patterns, and X-ray crystallographic file (CIF). This material is available free of charge via the Internet at http://pubs.acs.org.

IC8003855

(29) The powder X-ray diffraction patterns of evacuated **5** and **6** have shown significant peak broadening (Figure S4 in the Supporting Information), but the diffraction peaks of **5** are sharper than those of **6**. This result is consistent with the higher framework stability of **5**.